Intracellular distribution of bis-allylic deuterated linoleic acid into the lipidome of human keratinocytes

Rosangela S. Santos [a,1], Márcia S.F. Franco [a,1], Felipe G. Ravagnani [a,2], Adriano B. Chaves-Filho [a], Sayuri Miyamoto [a], Mauricio S. Baptista [a], Mikhail S. Shchepinov [b,**], Marcos Y. Yoshinaga [a,*,1]

[a] Institute of Chemistry, Department of Biochemistry – University of São Paulo, São Paulo, Brazil
[b] Retrotope, Inc., Los Altos, CA, USA

ARTICLE INFO

ABSTRACT

Polyunsaturated fatty acids (PUFA) are particularly susceptible to free radical-induced lipid peroxidation (LPO). Specific deuteration at bis-allylic positions of PUFA (D-PUFA) has been recently proposed as a way to inhibit the LPO. Here, a high mass resolution untargeted lipidomic analysis protocol was applied to examine the changes in the lipidome of keratinocytes supplemented with bis-allylic deuterated linoleic acid (D_2-LA). Incorporation of D_2-LA occurs preferentially in membrane phospholipids such as phosphatidylcholine and phosphatidylethanolamine, followed by triglycerides. However, the relative contribution of D_2-LA among membrane lipids is highest in cardiolipin (60%) followed by its precursor phosphatidylglycerol (50%). Cardiolipins are enriched in PUFA and exclusively located in mitochondrial membranes, thus representing major targets for lipid peroxidation. These findings indicate that D_2-LA supplementation is linked to the preservation of mitochondrial function under oxidative stress. Finally, our study highlights the suitability of high mass resolution lipidomic analysis to investigate lipid metabolism at the level of individual molecular species in stable isotope tracing experiments.

1. Introduction

Polyunsaturated fatty acids (PUFA) are essential components of membrane lipids of eukaryotes. PUFA are particularly relevant to the normal cellular function and bioenergetics, representing a significant proportion of fatty acids esterified to membrane lipids of chloroplasts, mitochondria, retina, and neurons (including synaptic vesicles) [1–5]. On the other hand, PUFA are highly susceptible to lipid peroxidation (LPO) through redox imbalance (or oxidative stress), which is a common feature of many human pathological conditions (e.g. atherosclerosis, neurological and age-dependent diseases [2,6,7]). The risk of LPO is linked to the formation of lipid radicals [8], thereby igniting a chain reaction that may extensively damage cellular membranes. If not controlled by potent antioxidant mechanisms, LPO can disrupt optimal membrane fluidity and permeability, thereby impairing the function of membrane-bound proteins and properties of cellular ion exchange [9–11], respectively. Moreover, the downstream products of LPO, such as

reactive carbonyls, are toxic to numerous biochemical pathways [12–14].

Since hydrogen abstraction from bis-allylic positions of PUFA is the rate-limiting step in lipid peroxidation [12], PUFA deuteration represents a conceivable strategy to counteract the cellular damages caused by excessive LPO. The rationale of PUFA deuteration is that hydrogen abstraction can be attenuated or inhibited by substituting hydrogen atoms at bis-allylic positions with deuterium (D-PUFA) [13] with the effect further multiplied by the chain nature of the LPO [14]. The effectiveness of D-PUFA treatment against LPO has been recently demonstrated in multiple cellular and animal models [13–19], including protection against light-induced lipid peroxidation [20]. Moreover, the active role of D-PUFA against LPO has been confirmed with only a modest contribution of D-PUFA in bilayer membranes (estimated at <20% of total PUFA [14,21]). Nonetheless, the intracellular distribution of D-PUFA at the level of the hundreds of individual lipid molecules comprising the cellular lipidome was not yet evaluated. The relative

---

* Corresponding author.
** Corresponding author.
E-mail addresses: misha@retrotope.com (M.S. Shchepinov), marcosyukio@gmail.com (M.Y. Yoshinaga).
[2] Present Address: Sociedade Beneficente Israelita Brasileira Albert Einstein São Paulo, Brazil.
[1] These authors contributed equally.

distribution of D-PUFA into storage and/or membrane lipids will surely complement the current understanding about the mechanisms of action of D-PUFA supplementation.

Herein, the fates of bis-allylic deuterated linoleic acid (11,11 D_2-LA) supplementation in the lipidome of keratinocytes were investigated by untargeted lipidomics using liquid chromatography coupled to high-resolution mass-spectrometry (LC-HRMS). For comparison, D_2-LA supplementation to cells was studied in parallel to additions of vehicle (BSA), oleic and linoleic acids. In addition, photosensitization experiments using a mitochondrial photosensitizer (di-methyl methylene blue) were performed to evaluate whether the supplementation with D_2-LA is able to protect mitochondria from oxidative stress.

2. Material and methods

2.1. Cell cultivation and lipid supplementation

Human nonmalignant immortalized keratinocytes HaCaT cells were seeded in 6-well plates (104 cells/cm^2) two days before the fatty acid (FA) incubations. Dulbecco Modified Eagle Medium (DMEM; Sigma-Aldrich, D5648), supplemented with FA-free bovine serum albumin (BSA; Gibco™, 12657029) was employed for fatty acid delivery (6:1 ratio for FA:BSA). For each experiment, 25 μM of FA (oleic, linoleic and D_2-LA) was added into the cell culture medium. DMEM with BSA was used as control for vehicle and non-deuterated oleic and linoleic acids were used as references for FA uptake. Twenty-four hours after BSA or FA-BSA incubations, cells were treated with trypsin and their respective pellets were maintained in ultra-freezer (-80 °C) until lipidomics analysis.

2.2. Lipid extraction and liquid chromatography tandem mass spectrometry analysis

Cell pellets were homogenized in 600 μL of 10 mM phosphate buffer (pH 7.4) containing 100 μM of deferoxamine mesylate as chelating agent. The homogenates were divided into 500 μL for lipid extraction and 100 μL for total protein quantification using BCA protein assay, according to manufacturer's instructions. The lipid extraction followed the protocol by Yoshida et al. [22] with slight modifications. To the 500 μL homogenates, 100 μL of a mix containing internal standards (detailed in Table S1) was added together with 300 μL of methanol. To these mixtures, 4 mL of chloroform:ethyl acetate (4:1) were added and the samples were thoroughly vortexed for 1 min. Samples were then sonicated for 20 min in ice bath and thereafter centrifuged (1500 g for 6 min at 4 °C). The lower phase containing the total lipid extract (TLE) was transferred to a new tube, evaporated to dryness under N_2 gas, and re-dissolved in 100 μL of isopropanol. The TLEs were measured by liquid chromatography (C18 column, reverse-phase) tandem electrospray time-of-flight mass spectrometry and the injection volume was set at 1 μL. For the untargeted lipidomic analysis a high-resolution electrospray time-of-flight mass spectrometer (ESI-TOFMS, Triple TOF 6600, Sciex) was used in tandem with an ultra high-performance liquid chromatography system (UHPLC Nexera, Shimadzu), as previously described [23]. One sample from each treatment (BSA, oleic, linoleic and D_2-LA) was randomly selected for lipid identification by MS/MS experiments. The top 300 most abundant ions from MS/MS experiments in each negative and positive ionization modes were manually annotated exclusively based on their fragmentation pattern (except for free fatty acids and free cholesterol). Thereby a list of exact masses and retention time for lipid species was generated and compounds were quantified as peak area in MS1 (see Table S1). Peak areas of lipid species were compared to those of the respective internal standard class (semi-quantitative approach), and the molar concentration for each lipid calculated and thereafter normalized by total protein concentrations. Finally, a pooled sample containing a 30 μL aliquot of TLE from each experimental sample was used as quality control. This pooled sample was injected before and after a batch of 5 experimental samples and the coefficient of variance (CV) was calculated.

2.3. Photosensitization with di-methyl methylene blue (DMMB) and cell viability

Keratinocytes were seeded in 96-well plates with growth medium 48 h before the photosensitization experiments at a density of 1×10^4 cells per well. The growth medium was removed 24 h prior to the experiments, washed once with PBS and filled with an equal volume of the supplemented medium containing 25 μM of FA (oleic, linoleic or D_2-LA). The supplemented DMEM medium containing FA was prepared according to the protocol described above, with FA-free BSA used as control for vehicle. Cells were washed with PBS and incubated with 10 nM DMMB for 1 h in a 37 °C incubator under a moist atmosphere of 5% carbon dioxide. DMMB treated cells were washed twice with PBS. Irradiation was carried out with Ethik with red LED with a maximum emission wavelength at 657 nm. To achieve 12 J cm^{-2}, cells were irradiated for 9 min at an irradiance of 23.5 Wm.cm^{-2}. Photosensitized and non-photosensitized cells maintained in PBS were used as DMMB-free controls.

Cell viability was estimated by measuring the reduction of resazurin into resorufin as product [24]. Photosensitized and non-photosensitized keratinocytes were washed with PBS and incubated with medium 1% (v:v) FBS containing AquaBluer™ for 4 h in a 37 °C incubator under a moist atmosphere of 5% carbon dioxide. Next, the plates were removed from incubator, and values were read in a fluorescence plate reader at 540 nm exposition and 590 nm emission, using SpectraMax i3 (Molecular Devices, USA). Cell viability for DMMB experiments (i.e. non-photosensitized and photosensitized cells) was calculated by normalizing the reads to the mean of their respective DMMB-free BSA controls [25].

2.4. Statistical analyses

Lipids concentrations were converted into molar per total protein content, and data are presented as mean ± standard deviation. Prior to statistical analysis, compounds displaying a CV >20% were excluded and the lipidomic data were log-transformed to achieve normal distribution. For univariate analysis, a one-way ANOVA was applied with a false discovery rate (FDR; as control of Type-I error or false positives) followed by a post-hoc Tukey's test to identify differences between treatments, and a p value of <0.05 was adopted for significance. Statistical analyses were conducted using Metaboanalyst (www.metaboanalyst.ca), following protocols in Pang et al. [26]. Statistical analysis for cell viability in photosensitization experiments was performed in GraphPrism.

3. Results

The m/z resemblance between oleic acid (18:1) and 11,11 D_2-LA (D18:2) is one of the major challenges in evaluating D-PUFA incorporation into cellular lipidome. Fortunately, untargeted lipidomics by LC-HRMS allowed not only to distinguish MS/MS fragment ions derived from D_2-LA and oleic acid, which display a 3 mDa mass difference, but also to quantify compounds of very similar masses with suitable baseline separation (Fig. 1; Fig. S2). As an example, two phosphatidylcholine (PC) linked to palmitate (16:0) and either D_2-LA or oleic, both having a m/z of 818.5917 ± 5mDA, were successfully identified not just based on the m/z difference between D_2-LA and oleic acid, but also given the optimal separation by liquid chromatography (i.e. distinct retention times of 9.18 and 9.61 min; Fig. 1A). Similarly, triglycerides (TG) from cells treated with BSA or supplemented with D_2-LA having a m/z 874.7858 ± 5mDA, but containing natural isotopes or 11,11 D_2-LA, respectively, could be unequivocally identified based on m/z of fragments in MS/MS experiments and distinct retention times (Fig. 1D).

A total of 309 individual lipid species were identified, from these 206 comprising natural isotopes and 103 species containing D_2-LA in their structure (Table S1). The numerical contribution of D_2-LA containing species to the total number of lipids within a single class is shown in
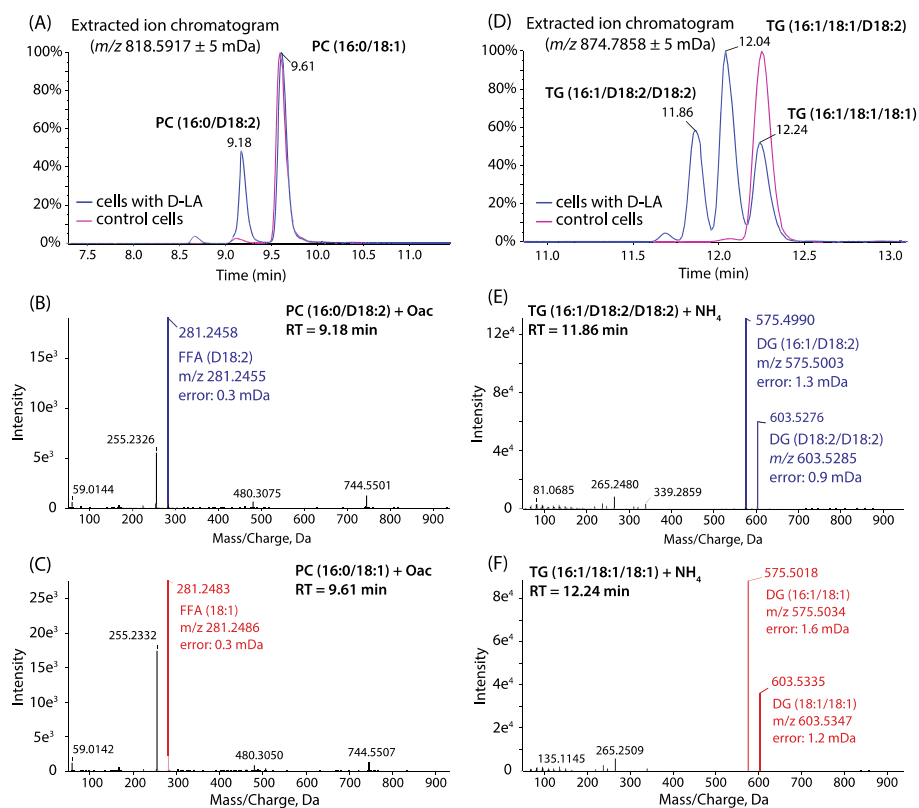
Fig. 1. **Identification of phosphatidylcholine (PC) and triglyceride (TG) species containing D₂-LA (D18:2) and natural isotopes by LC-HRMS from a sample supplemented with D₂-LA (blue) and a BSA control sample (red).** Total ion chromatograms of precursor ions m/z 818.59 (A) and m/z 874.78 (D) showing baseline separation of PC and TG species, respectively. B and C) Negative ionization mode MS/MS chromatograms of PC (16:0/D18:2) and PC (16:0/18:1), respectively, displaying fatty acid (FA) fragments ions from D18:2 and 18:1. E and F) Positive ionization mode MS/MS chromatograms of TG (16:1/D18:2/D18:2) and TG (16:1/18:1/18:1), respectively, displaying fragments of diacylglycerides (DG). Theoretical masses of FA (B and C) and DG (E and F) are displayed and compared to experimental masses (errors are indicated). Please see Fig. S1 for details in the structures of these lipids. (For interpretation of the references to color in this figure legend, the reader is referred to the Web version of this article.)

Table S1. Of note, and although comprising only a small fraction of total lipids, elongated products of D₂-LA were observed as free fatty acids (FFA) and n-acyl chains of sphingolipids with 20, 22 and 24 carbons (Table S1; Fig. S3).

The addition of fatty acids (25 μM) to keratinocytes (D₂-LA, oleic and linoleic acids) did not stimulate major alterations in the concentrations of lipid classes as compared to the vehicle (BSA), except for a trend of increased concentrations in neutral lipids, particularly glycerolipids (Fig. S3). Notably, D₂-LA was incorporated into multiple lipid classes, and D₂-LA containing species represented in average ca. 23% of total lipid concentrations (Fig. 2A and S3).

Among neutral lipids, D₂-LA was mainly esterified to triglycerides (TG), representing ca. 26% of total D₂-LA incorporation, followed by alkyl-diacylglycerols (ADG) and cholesteryl esters (CE) to a minor extent (Fig. 2B). Among glycerophospholipids, phosphatidylcholine (PC) and phopshatidylethanolamine (PE) displayed by far the highest content of D₂-LA, together representing ca. 60% of total D₂-LA incorporation, whereas phosphatidylinositol (PI), cardiolipin (CL) and phosphatidylglycerol (PG) comprised only a small fraction of D₂-LA (Fig. 2B). Although contributing less than 5% of total incorporation, D₂-LA was also
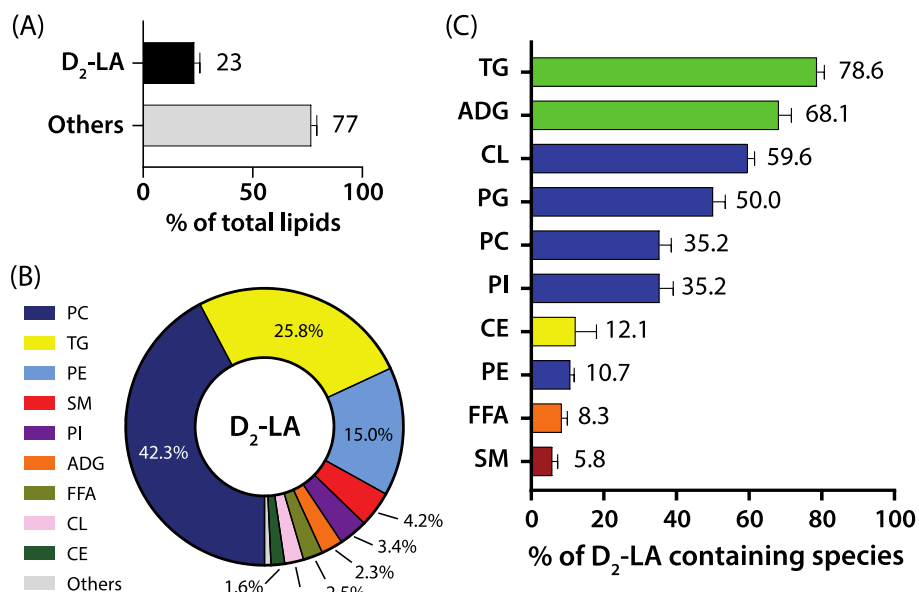

Fig. 2. **Analysis of D₂-LA incorporation into the lipidome of keratinocytes**. A) Total contribution of D₂-LA for the sum of lipids described and quantified in this study. B) Quantitative data displaying the relative abundance of D₂-LA incorporation into several lipid classes (please see text for abbreviations). C) Relative data showing the highest contributions of D₂-LA containing species for lipid classes. Bars are color coded as: glycerolipids (green), glycerophospholipids (blue), sterols (yellow), free fatty acids (orange) and sphingolipids (red). Data is presented as the mean ± standard deviation of triplicates. Please see text for abbreviations. (For interpretation of the references to color in this figure legend, the reader is referred to the Web version of this article.)

observed in n-acyl chains of both sphingomyelins (SM) and ceramides (Cer).

Apart from the quantitative data on D_2-LA incorporation among lipid classes, our findings revealed very distinct contributions of D_2-LA containing species to the total lipid concentrations within a specific class. For example, among neutral lipids, D_2-LA containing species represented 80 and 70% of all TG and ADG, respectively, whereas their contribution to CE was only 12% (Fig. 2C). In glycerophospholipids, D_2-LA containing species represented 60 and 50% of total CL and PG concentrations, followed by ca. 35% of PC and PI, and only 11% in PE (Fig. 2C). For other lipid classes such as FFA and sphingolipids, D_2-LA containing species contributed less than 10% of total concentrations.

Interestingly, the analysis of the relative abundance of individual fatty acids within a single lipid class allowed to investigate the effects of D_2-LA, OA and LA supplementation in the contribution of saturated (SFA), monounsaturated (MUFA) and polyunsaturated (PUFA) fatty acids within major glycerolipids and phosphoglycerolipids (Fig. 3). The results revealed a consistently lower contribution of MUFA in major lipid classes of D_2-LA treated cells as compared to control and other treatments (Fig. 3B). More specifically, our data showed that D_2-LA consistently substituted for oleic acid, rather than linoleic acid or any other PUFA (Fig. 3).

The highest contribution of D_2-LA containing species among CL and PG, two membrane lipids exclusively found in mitochondria [27], prompted the investigation of PUFA deuteration against photooxidative damage targeting keratinocytes mitochondria. For this purpose, keratinocytes were incubated with DMMB at 10 nM, to induce photooxidative damage specifically in mitochondrial membranes during and after light exposure [28]. As shown in Fig. 4, despite the variability in non-photosensitized cells, irradiation with DMMB led to a considerable decrease in cell viability of keratinocytes in both controls (BSA, oleic and linoleic acids) and D_2-LA treatments. More importantly, the results also revealed that D_2-LA addition was the only fatty acid treatment that effectively protected cells against irradiation with DMMB, displaying higher cell viability as compared to BSA (Fig. 4B).

4. Discussion

Our study provided data not only on species-specific incorporation of D_2-LA, but also its potential metabolic fates. For instance, D_2-LA as FFA and N-linked acyl chains of sphingolipids was found elongated with addition of 2–6 carbons (Table S1; Fig. S3). Despite the latter evidence for the action of elongases, products of D_2-LA desaturation were not apparent in the pools of glycerolipids or glycerophospholipids, as well as shorter carbon chain products derived from fatty acid β-oxidation were not detected by our methods. At least for cultured keratinocytes, D_2-LA appeared to function as a surrogate for oleic acid rather than PUFA in several lipid classes (Fig. 3). Nonetheless, the likelihood of desaturases activity on D_2-LA cannot be ruled out for other cell types or at the whole organism level. The possibility to monitor the fate of D-PUFA in hundreds of lipid molecular species using LC/HRMS widens the opportunities for designing specific PUFA deuteration as surrogates for the protection of cellular lipidome against oxidative stress.

The goal of this study was to comprehensively access the dynamics of D_2-LA incorporation into the cellular lipidome of human keratinocytes. Our data revealed that D_2-LA containing lipids represented 23% of total lipid concentrations, a ballpark reported to stop lipid peroxidation in other studies [17,29]. The phospholipids PC and PE represented together more than 60% of the total D_2-LA incorporation, followed by TG species with 26%. Certainly, these bulk quantitative figures in D_2-LA supplementation may change with other cell types and metabolic conditions. Notably our findings revealed a very distinct contribution of D_2-LA containing lipid species within individual classes. The contributions of D_2-LA containing species to TG and ADG were estimated at 80 and 70% of the total concentrations, respectively. While confined to lipid droplets, both TG and ADG are likely protected from aqueous pro-oxidants and
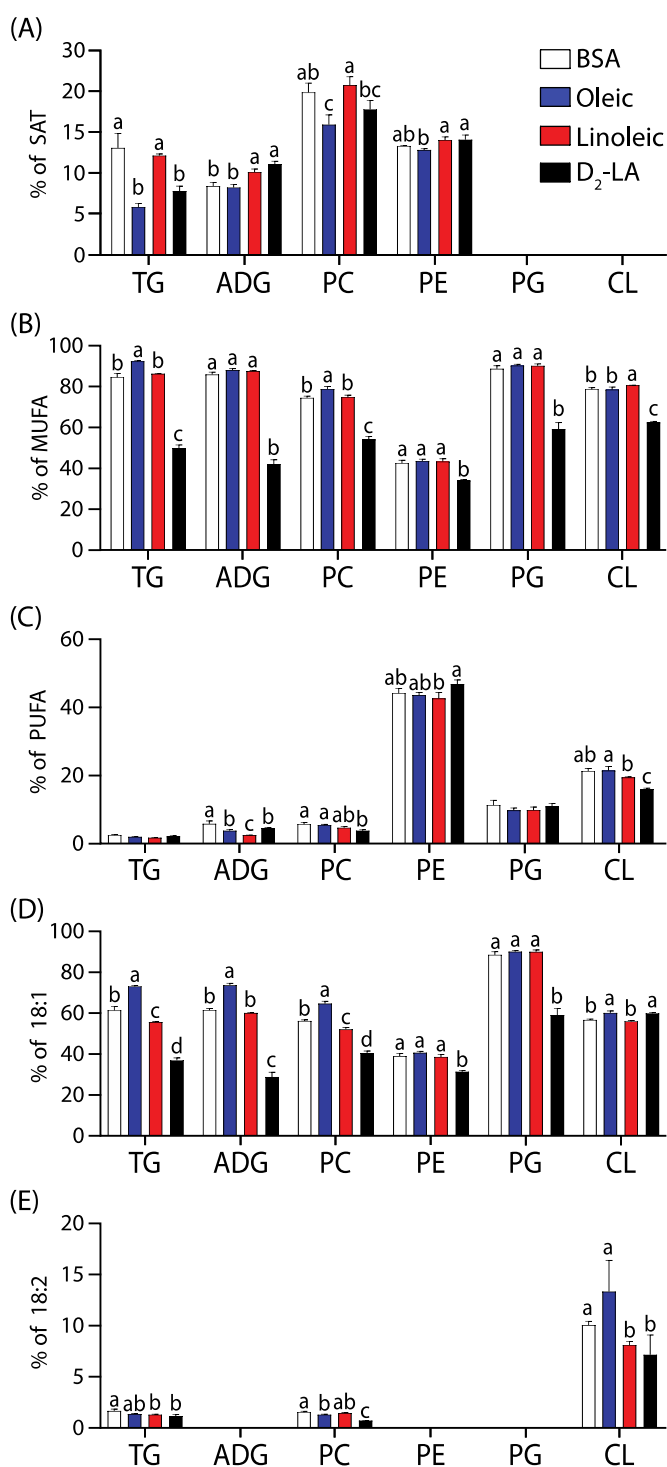

Fig. 3. Relative contributions of fatty acids for selected glycerolipids and glycerophospholipids from keratinocytes supplemented with D_2-LA and controls (BSA, oleic and linoleic acids). Fatty acids were categorized as (A) saturated (SAT), (B) monounsaturated (MUFA) and (C) polyunsaturated (PUFA) fatty acids. D_2-LA was not included in PUFA percentage. Oleic (D) and linoleic (E) acids are also displayed. Data is presented as the mean ± standard deviation of triplicates. Means not sharing a common letter above bars are significantly different from each other, $p < 0.05$.

chain reactions occurring at cellular membranes [23,30]. Alternatively, as storage lipids, D_2-LA can be readily hydrolyzed from TG and ADG providing not just fuel for β-oxidation in events of nutrient deprivation
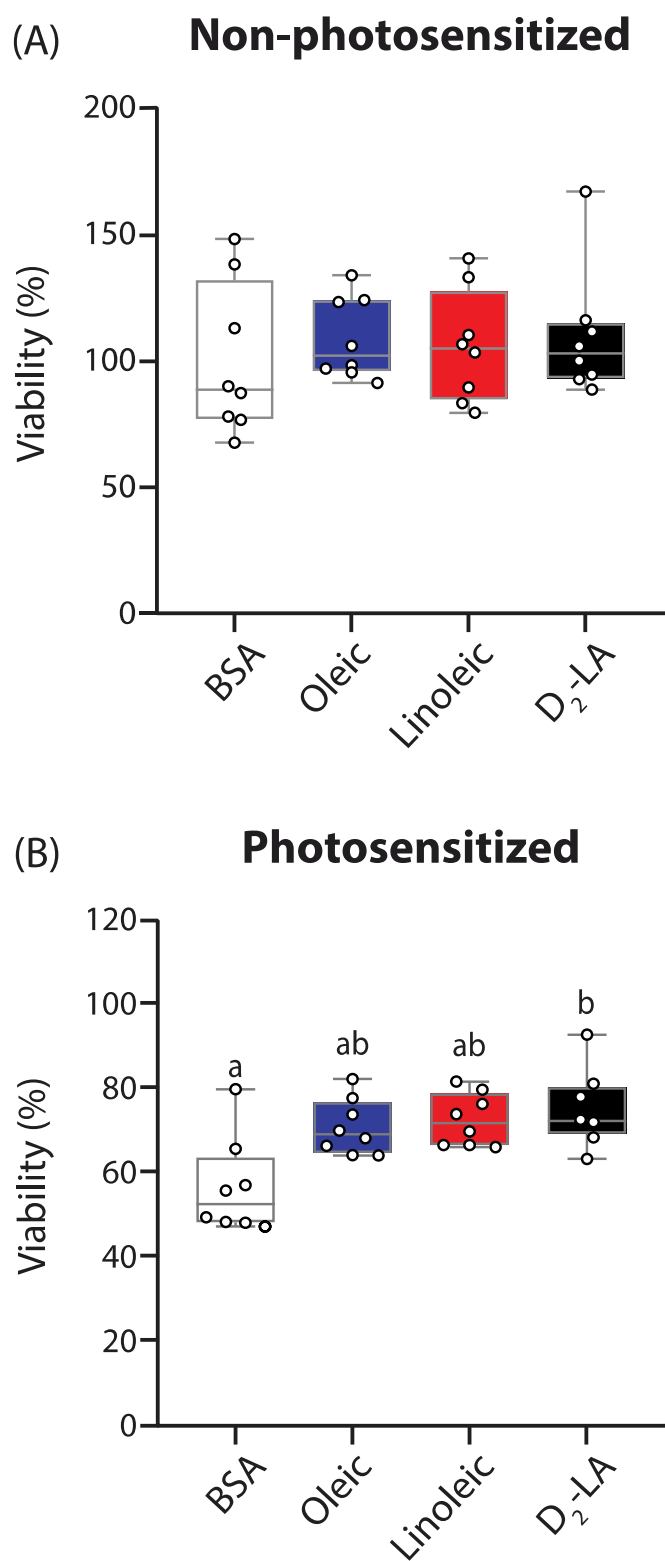
(A) Non-photosensitized

(B) Photosensitized

Fig. 4. Effects of irradiation using di-methyl methylene blue (DMMB) on the cell viability of keratinocytes supplemented with D_2-LA and controls (n = 8). Both non-photosensitized (A) and photosensitized (B) keratinocytes were incubated with DMMB and cell viability estimated in percentage against DMMB-free controls. Data is presented as the mean ± standard deviation of replicates. Means not sharing a common letter above bars are significantly different from each other, p < 0.05. (For interpretation of the references to color in this figure legend, the reader is referred to the Web version of this article.)

[31], but perhaps fatty acyl chains to repair damaged membranes undergoing excessive lipid peroxidation [32].

Interestingly, among membrane lipids, the highest contributions of D_2-LA containing species to the total concentrations of a single class were observed for CL and PG, two phospholipids uniquely located to mitochondria and particularly concentrated at their inner membranes [33, 34]. While displaying a high content of D_2-LA and comprising together more than 50% of all mitochondrial lipids, PC and PE, in contrast to CL and PG, are not exclusively located at mitochondria [27]. PG is a precursor in the synthesis of CL, a dimeric phospholipid with four acyl chains that make up 20% of the total phospholipids in mitochondrial inner membranes [27]. The essential nature of CL for mitochondrial function has been extensively demonstrated, including structural (membrane curvature, formation/stabilization of protein complexes [35–38]), bioenergetics (e.g. as proton wells [39,40]), dynamics (fission/fusion [41]) and signaling roles (apoptosis, mitophagy, inflammation [42–44]). Several diseases associated with mitochondrial dysfunction are characterized by changes in the content of CL, including Barth syndrome [45] and others such as diabetes and cardiovascular diseases [46]. In addition, attention has been recently given to the role of CL acyl chains remodeling, which consists in the enrichment of PUFA, as important trait affecting mitochondrial morphology and function [47]. Since CL-linked PUFA peroxidation is putatively considered as key signal for the apoptotic cascade [43,48], efficient repairing and remodeling of CL acyl chains for protection under pathological conditions are critical for normal cell physiology.

Although the therapeutic potential of D-PUFA has been previously attributed to the preservation of mitochondrial function [19], the mechanistic details of D-PUFA associated protection are yet to be fully elucidated [49]. Nonetheless, D-PUFA have been shown to reduce both the progression of light-triggered and dark lipid peroxidation reactions [50]. In concert with the lipidomic data, D_2-LA supplementation to keratinocytes was the only fatty acid treatment to yield higher cell viability relative to the vehicle BSA in photosensitization experiments with DMMB – a photosensitizer targeted to damage mitochondrial membranes [28].

Collectively, the preferential enrichment of CL and PG with D_2-LA as compared to other membrane lipid classes (e.g. sphingolipids or PC and PE) and the protection of D-PUFA treated keratinocytes against photooxidative damage targeted to mitochondria are consistent with the hypothesis of D-PUFA assisted reduction in lipid peroxidation occurring at the level of mitochondrial membranes [19]. Moreover, the availability of D_2-LA in the pools of ADG and TG may render cells with a large reservoir of acyl chains for repairing damaged membranes [32]. Finally, our study reinforces the suitability of applying untargeted lipidomic analysis using LC/HRMS for stable isotope tracing experiments, especially when D-PUFA containing lipids (with addition of few deuterium atoms) have very similar masses as compared to their natural isotope counterparts.

Notes

Declaration of competing interest

The authors declare that they have no known competing financial interests or personal relationships that could have appeared to influence the work reported in this paper.

Acknowledgements

Higher Education Personnel (CAPES); CEPID Redoxoma (13/07937–8) by Sao Paulo Research Foundation (FAPESP).

Appendix A. Supplementary data

Supplementary data to this article can be found online at https://doi.org/10.1016/j.rbc.2023.100005.

References

[1] R.C. Valentine, D.L. Valentine, Omega-3 fatty acids in cellular membranes: a unified concept, Prog. Lipid Res. 43 (5) (2004) 383–402, https://doi.org/10.1016/J.PLIPRES.2004.05.004.

[2] R.C. Valentine, D.L. Valentine, Human longevity: omega-3 fatty acids, bioenergetics, molecular biology, and evolution. *Human longevity: omega-3 fatty acids*, Bioenerget. Mol. Biol. Evol. (2014) 1–228, https://doi.org/10.1201/B17458/HUMAN-LONGEVITY-RAYMOND-VALENTINE-DAVID-VALENTINE.

[3] T. Botana, M. Chaves-Filho, A.B. Inague, A.Z. Güth, A. Saldanha-Corrêa, F. Müller, M.N. Sumida, P.Y.G. Miyamoto, S. Kellermann, M.Y. Valentine, R.C. Yoshinaga, M, Y, Thermal plasticity of coral reef symbionts is linked to major alterations in their lipidome composition, Limnol. Oceanogr. 67 (7) (2022) 1456–1469, https://doi.org/10.1002/LNO.12094.

[4] S. Takamori, M. Holt, K. Stenius, E.A. Lemke, M. Grønborg, D. Riedel, H. Urlaub, S. Schenck, B. Brügger, P. Ringler, S.A. Müller, B. Rammner, F. Gräter, J.S. Hub, B.L. de Groot, G. Mieskes, Y. Moriyama, J. Klingauf, H. Grubmüller, J. Heuser, F. Wieland, R. Jahn, Molecular anatomy of a trafficking organelle, Cell 127 (4) (2006) 831–846, https://doi.org/10.1016/J.CELL.2006.10.030.

[5] T. Harayama, T. Shimizu, Roles of polyunsaturated fatty acids, from mediators to membranes, J. Lipid Res. 61 (8) (2020) 1150–1160, https://doi.org/10.1194/JLR.R120000800.

[6] M.T. Lin, M.F. Beal, Mitochondrial dysfunction and oxidative stress in neurodegenerative diseases, Nature 443 (7113) (2006) 787–795, https://doi.org/10.1038/nature05292, 2006 443:7113.

[7] G. Pizzino, N. Irrera, M. Cucinotta, G. Pallio, F. Mannino, V. Arcoraci, F. Squadrito, D. Altavilla, A. Bitto, Oxidative stress: harms and benefits for human health, Oxid. Med. Cell. Longev. 2017 (2017), https://doi.org/10.1155/2017/8416763.

[8] H. Yin, L. Xu, N.A. Porter, Free radical lipid peroxidation: mechanisms and analysis, Chem. Rev. 111 (10) (2011) 5944–5972, https://doi.org/10.1021/CR200084Z/ASSET/CR200084Z.FP.PNG_V03.

[9] M.E. Greenberg, X.M. Li, B.G. Gugiu, X. Gu, J. Qin, R.G. Salomon, S.L. Hazen, The lipid whisker model of the structure of oxidized cell membranes, J. Biol. Chem. 283 (4) (2008) 2385–2396, https://doi.org/10.1074/JBC.M707348200.

[10] Á. Catalá, Lipid peroxidation modifies the assembly of biological membranes "the lipid whisker model.", Front. Physiol. 6 (JAN) (2015) 520, https://doi.org/10.3389/FPHYS.2014.00520/BIBTEX.

[11] I.O.L. Bacellar, M.S. Baptista, Mechanisms of photosensitized lipid oxidation and membrane permeabilization, ACS Omega 4 (26) (2019) 21636–21646, https://doi.org/10.1021/ACSOMEGA.9B03244/ASSET/IMAGES/LARGE/AO9B03244_0001.JPEG.

[12] J.P.F. Angeli, C.C.M. Garcia, F. Sena, F.P. Freitas, S. Miyamoto, M.H.G. Medeiros, P. di Mascio, Lipid hydroperoxide-induced and hemoglobin-enhanced oxidative damage to colon cancer cells, Free Radic. Biol. Med. 51 (2) (2011) 503–515, https://doi.org/10.1016/J.FREERADBIOMED.2011.04.015.

[13] J. Mano, Reactive carbonyl species: their production from lipid peroxides, action in environmental stress, and the detoxification mechanism, Plant Physiol. Biochem. 59 (2012) 90–97, https://doi.org/10.1016/J.PLAPHY.2012.03.010.

[14] M.S. Biswas, J. Mano, Lipid peroxide-derived reactive carbonyl species as mediators of oxidative stress and signaling, Front. Plant Sci. 12 (2021) 2400, https://doi.org/10.3389/FPLS.2021.720867/BIBTEX.

[15] B.A. Wagner, C.P. Burns, G.R. Buettner, Free radical-mediated lipid peroxidation in cells: oxidizability is a function of cell lipid bis-allylic hydrogen content, Biochemistry 33 (15) (1994) 4449–4453, https://doi.org/10.1021/BI00181A003.

[16] S. Hill, K. Hirano, V.v. Shmanai, B.N. Marbois, D. Vidovic, A.v. Bekish, B. Kay, V. Tse, J. Fine, C.F. Clarke, M.S. Shchepinov, Isotope-reinforced polyunsaturated fatty acids protect yeast cells from oxidative stress, Free Radic. Biol. Med. 50 (1) (2011) 130–138, https://doi.org/10.1016/J.FREERADBIOMED.2010.10.690.

[17] S. Hill, C.R. Lamberson, L. Xu, R. To, H.S. Tsui, V.v. Shmanai, A.v. Bekish, A.M. Awad, B.N. Marbois, C.R. Cantor, N.A. Porter, C.F. Clarke, M.S. Shchepinov, Small amounts of isotope-reinforced polyunsaturated fatty acids suppress lipid autoxidation, Free Radic. Biol. Med. 53 (4) (2012) 893–906, https://doi.org/10.1016/J.FREERADBIOMED.2012.06.004.

[18] J.F.P. Berbée, I.M. Mol, G.L. Milne, E. Pollock, G. Hoeke, D. Lütjohann, C. Monaco, P.C.N. Rensen, L.H.T. van der Ploeg, M.S. Shchepinov, Deuterium-reinforced polyunsaturated fatty acids protect against atherosclerosis by lowering lipid peroxidation and hypercholesterolemia, Atherosclerosis 264 (2017) 100–107, https://doi.org/10.1016/J.ATHEROSCLEROSIS.2017.06.916.

[19] A.Y. Andreyev, H.S. Tsui, G.L. Milne, V.v. Shmanai, A.v. Bekish, M.A. Fomich, M.N. Pham, Y. Nong, A.N. Murphy, C.F. Clarke, M.S. Shchepinov, Isotope-reinforced polyunsaturated fatty acids protect mitochondria from oxidative stress, Free Radic. Biol. Med. 82 (2015) 63–72, https://doi.org/10.1016/J.FREERADBIOMED.2014.12.023.

[20] S.M. Raefsky, R. Furman, G. Milne, E. Pollock, P. Axelsen, M.P. Mattson, M.S. Shchepinov, Deuterated polyunsaturated fatty acids reduce brain lipid peroxidation and hippocampal amyloid β-peptide levels, without discernible behavioral effects in an APP/PS1 mutant transgenic mouse model of alzheimer's disease, Neurobiol. Aging 66 (2018) 165–176, https://doi.org/10.1016/J.NEUROBIOLAGING.2018.02.024.

[21] M. Rosell, M. Giera, P. Brabet, M.S. Shchepinov, M. Guichardant, T. Durand, J. Vercauteren, J.M. Galano, C. Crauste, Bis-allylic deuterated DHA alleviates oxidative stress in retinal epithelial cells, Antioxidants 8 (10) (2019), https://doi.org/10.3390/ANTIOX8100447.

[22] Y. Yoshida, S. Kodai, S. Takemura, Y. Minamiyama, E. Niki, Simultaneous measurement of F_2-isoprostane, hydroxyoctadecadienoic acid, hydroxyeicosatetraenoic acid, and hydroxycholesterols from physiological samples, Anal. Biochem. 379 (1) (2008) 105–115, https://doi.org/10.1016/j.ab.2008.04.028.

[23] A.B. Chaves-Filho, I.F.D. Pinto, L.S. Dantas, A.M. Xavier, A. Inague, R.L. Faria, M.H.G. Medeiros, I. Glezer, M.Y. Yoshinaga, S. Miyamoto, Alterations in lipid metabolism of spinal cord linked to amyotrophic lateral sclerosis, Sci. Rep. 9 (1) (2019), 11642, https://doi.org/10.1038/s41598-019-48059-7.

[24] S.N. Rampersad, Multiple applications of alamar blue as an indicator of metabolic function and cellular health in cell viability bioassays, Sensors 12 (9) (2012) 12347–12360, https://doi.org/10.3390/S120912347, 2012, Vol. 12, Pages 12347-12360.

[25] A.F.L. Specian, J.M. Serpeloni, K. Tuttis, D.L. Ribeiro, H.L. Cilião, E.A. Varanda, M. Sannomiya, W. Martinez-Lopez, I.M.S. Cólus, LDH, proliferation curves and cell cycle analysis are the most suitable assays to identify and characterize new phytotherapeutic compounds, Cytotechnology 68 (6) (2016) 2729–2744, https://doi.org/10.1007/S10616-016-9998-6/FIGURES/6.

[26] Z. Pang, G. Zhou, J. Ewald, L. Chang, O. Hacariz, N. Basu, J. Xia, Using MetaboAnalyst 5.0 for LC–HRMS spectra processing, multi-omics integration and covariate adjustment of global metabolomics data, Nat. Protoc. 17 (2022) 1735–1761, https://doi.org/10.1038/s41596-022-00710-w.

[27] S.E. Horvath, G. Daum, Lipids of mitochondria, Prog. Lipid Res. 52 (4) (2013) 590–614, https://doi.org/10.1016/J.PLIPRES.2013.07.002.

[28] W.K. Martins, N.F. Santos, C. de S. Rocha, I.O.L. Bacellar, T.M. Tsubone, A.C. Viotto, A.Y. Matsukuma, A.B. de P. Abrantes, P. Siani, L.G. Dias, M.S. Baptista, Parallel damage in mitochondria and lysosomes is an efficient way to photoinduce cell death, Autophagy 15 (2) (2019) 259–279, https://doi.org/10.1080/15548627.2018.1515609.

[29] A.M. Firsov, M.A. Fomich, A.v. Bekish, O.L. Sharko, E.A. Kotova, H.J. Saal, D. Vidovic, V.v. Shmanai, D.A. Pratt, Y.N. Antonenko, M.S. Shchepinov, Threshold protective effect of deuterated polyunsaturated fatty acids on peroxidation of lipid bilayers, FEBS J. 286 (11) (2019) 2099–2117, https://doi.org/10.1111/FEBS.14807.

[30] A.P. Bailey, G. Koster, C. Guillermier, E.M.A. Hirst, J.I. MacRae, C.P. Lechene, A.D. Postle, A.P. Gould, Antioxidant role for lipid droplets in a stem cell niche of Drosophila, Cell 163 (2) (2015) 340–353, https://doi.org/10.1016/J.CELL.2015.09.020.

[31] T. Petan, E. Jarc, M. Jusović, Lipid droplets in cancer: guardians of fat in a stressful world, Molecules 23 (8) (2018) 1941, https://doi.org/10.3390/MOLECULES23081941, 2018, Vol. 23, Page *1941*.

[32] J. Girón-Calle, P.C. Schmid, H.H.O. Schmid, Effects of oxidative stress on glycerolipid acyl turnover in rat hepatocytes, Lipids 32 (9) (1997) 917–923, https://doi.org/10.1007/S11745-997-0118-9.

[33] M. Ren, C.K.L. Phoon, M. Schlame, Metabolism and function of mitochondrial cardiolipin, Prog. Lipid Res. 55 (1) (2014) 1–16, https://doi.org/10.1016/J.PLIPRES.2014.04.001.

[34] E.M. Mejia, H. Nguyen, G.M. Hatch, Mammalian cardiolipin biosynthesis, Chem. Phys. Lipids 179 (2014) 11–16, https://doi.org/10.1016/J.CHEMPHYSLIP.2013.10.001.

[35] R.N.A.H. Lewis, R.N. McElhaney, The physicochemical properties of cardiolipin bilayers and cardiolipin-containing lipid membranes, Biochim. Biophys. Acta 1788 (10) (2009) 2069–2079, https://doi.org/10.1016/J.BBAMEM.2009.03.014.

[36] M. Zhang, E. Mileykovskaya, W. Dowhan, Cardiolipin is essential for organization of complexes III and IV into a supercomplex in intact yeast mitochondria, J. Biol. Chem. 280 (33) (2005) 29403–29408, https://doi.org/10.1074/JBC.M504951200.

[37] L.D. Renner, D.B. Weibel, Cardiolipin microdomains localize to negatively curved regions of Escherichia coli membranes, Proc. Natl. Acad. Sci. U. S. A. 108 (15) (2011) 6264–6269, https://doi.org/10.1073/PNAS.1015757108.

[38] N. Ikon, R.O. Ryan, Cardiolipin and mitochondrial cristae organization, Biochim. Biophys. Acta Biomembr. 1859 (6) (2017) 1156–1163, https://doi.org/10.1016/J.BBAMEM.2017.03.013.

[39] T.H. Haines, N.A. Dencher, Cardiolipin: a proton trap for oxidative phosphorylation, FEBS Lett. 528 (1–3) (2002) 35–39, https://doi.org/10.1016/S0014-5793(02)03292-1.

[40] M.Y. Yoshinaga, M.Y. Kellermann, D.L. Valentine, R.C. Valentine, Phospholipids and glycolipids mediate proton containment and circulation along the surface of energy-transducing membranes, Prog. Lipid Res. 64 (2016) 1–15, https://doi.org/10.1016/J.PLIPRES.2016.07.001.

[41] M.A. Frohman, Role of mitochondrial lipids in guiding fission and fusion, J. Mol. Med. (Berl.) 93 (3) (2015) 263–269, https://doi.org/10.1007/S00109-014-1237-Z.

[42] J. Dudek, Role of cardiolipin in mitochondrial signaling pathways, Front. Cell Dev. Biol. 5 (SEP) (2017) 90, https://doi.org/10.3389/FCELL.2017.00090/BIBTEX.

[43] V.E. Kagan, V.A. Tyurin, J. Jiang, Y.Y. Tyurina, V.B. Ritov, A.A. Amoscato, A.N. Osipov, N.A. Belikova, A.A. Kapralov, V. Kini, I.I. Vlasova, Q. Zhao, M. Zou, P. Di, D.A. Svistunenko, I.v. Kurnikov, G.G. Borisenko, Cytochrome c acts as a cardiolipin oxygenase required for release of proapoptotic factors, Nat. Chem. Biol. 1 (4) (2005) 223–232, https://doi.org/10.1038/nchembio727, 1:*4* 2005.

[44] C.T. Chu, J. Ji, R.K. Dagda, J.F. Jiang, Y.Y. Tyurina, A.A. Kapralov, V.A. Tyurin, N. Yanamala, I.H. Shrivastava, D. Mohammadyani, K.Z. Qiang Wang, J. Zhu, J. Klein-Seetharaman, K. Balasubramanian, A.A. Amoscato, G. Borisenko, Z. Huang, A.M. Gusdon, A. Cheikhi, E.K. Steer, R. Wang, C. Baty, S. Watkins, I. Bahar, H. Bayir, V.E. Kagan, Cardiolipin externalization to the outer mitochondrial membrane acts as an elimination signal for mitophagy in neuronal cells, Nat. Cell Biol. 15 (10) (2013) 1197–1205, https://doi.org/10.1038/ncb2837, 2013 15:10.

[45] P. Vreken, F. Valianpour, L.G. Nijtmans, L.A. Grivell, B. Plecko, R.J.A. Wanders, P.G. Barth, Defective remodeling of cardiolipin and phosphatidylglycerol in Barth syndrome, Biochem. Biophys. Res. Commun. 279 (2) (2000) 378–382, https:// doi.org/10.1006/BBRC.2000.3952.

[46] A.J. Chicco, G.C. Sparagna, Role of cardiolipin alterations in mitochondrial dysfunction and disease, Am. J. Physiol. Cell Physiol. 292 (1) (2007), https:// doi.org/10.1152/AJPCELL.00243.2006.

[47] E.R. Pennington, K. Funai, D.A. Brown, S.R. Shaikh, The role of cardiolipin concentration and acyl chain composition on mitochondrial inner membrane molecular organization and function, Biochim. Biophys. Acta Mol. Cell Biol. Lipids 1864 (7) (2019) 1039–1052, https://doi.org/10.1016/J.BBALIP.2019.03.012.

[48] H. Yin, M. Zhu, Free radical oxidation of cardiolipin: chemical mechanisms, detection and implication in apoptosis, Mitochon. Dysfunction and Human Dis. 46 (8) (2012) 959–974, https://doi.org/10.3109/10715762.2012.676642.

[49] M.S. Shchepinov, Polyunsaturated fatty acid deuteration against neurodegeneration, Trends Pharmacol. Sci. 41 (4) (2020) 236–248, https:// doi.org/10.1016/J.TIPS.2020.01.010.

[50] A.M. Firsov, M.S.F. Franco, D.v. Chistyakov, S.v. Goriainov, M.G. Sergeeva, E.A. Kotova, M.A. Fomich, A.v. Bekish, O.L. Sharko, V.v. Shmanai, R. Itri, M.S. Baptista, Y.N. Antonenko, M.S. Shchepinov, Deuterated polyunsaturated fatty acids inhibit photoirradiation-induced lipid peroxidation in lipid bilayers, J. Photochem. Photobiol., B 229 (2022), https://doi.org/10.1016/ J.JPHOTOBIOL.2022.112425.